Geophysical Journal International

Geophys. J. Int. (2014) **199,** 1166–1175
GJI Seismology

doi: 10.1093/gji/ggu318

Dynamic characteristics of an active coastal spreading area using ambient noise measurements—Anchor Bay, Malta

Pauline Galea, Sebastiano D'Amico and Daniela Farrugia

Physics Department, University of Malta, Msida MSD 2080*, Malta. E-mail: pauline.galea@um.edu.mt*

Accepted 2014 August 14. Received 2014 July 21; in original form 2014 February 5

SUMMARY

Anchor Bay and surrounding regions are located on the northwest coast of the island of Malta, Central Mediterranean. The area is characterized by a coastal cliff environment having an outcropping layer of hard coralline limestone (UCL) resting on a thick (up to 50 m) layer of clays and marls (Blue Clay, BC). This configuration gives rise to coastal instability effects, in particular lateral spreading phenomena and rock falls. Previous and ongoing studies have identified both lateral spreading rates and vertical motions of several millimetres per year. The area is an interesting natural laboratory as coastal detachment processes in a number of different stages can be identified and are easily accessible. We investigate the site dynamic characteristics of this study area by recording ambient noise time-series at more than 30 points, over an area of 0.07 km^2, using a portable three-component seismograph. The time-series are processed to give both horizontal-to-vertical spectral ratio graphs (H/V) as well as frequency-dependent polarisation analysis. The H/V graphs illustrate and quantify aspects of site resonance effects due both to underlying geology as well as to mechanical resonance of partly or wholly detached blocks. The polarization diagrams indicate the degree of linearity and predominant directions of vibrational effects. H/V curves closer to the cliff edge show complex responses at higher frequencies, characteristic of the dynamic behaviour of individual detached blocks. Particle motion associated with the higher frequencies shows strongly directional polarization and a high degree of linearity at well-defined frequencies, indicative of normal-mode vibration. The stable plateau areas, on the other hand, show simple, single-peak H/V curves representative of the underlying stratification and no predominant polarization direction. These results, which will be compared with those from other experiments in the area, have important implications for the understanding of ongoing processes in geologically active and unstable coastal environments.

Key words: Geomorphology; Geomechanics; Site effects; Wave propagation.

1 INTRODUCTION

Landslides and rockfalls present a significant geohazard, especially in areas of coastal instability. These are generally classified into a number of landslide mechanisms, such as rotational, translational and block sliding, rock toppling, debris flow, lateral spreading, etc., however a common cause of many of these failure types is the superposition of rock strata with different geomechanical properties and erosional characteristics (Gigli *et al.* 2012). An understanding of the mechanisms leading to slope failure is critical to assessing the hazard due to these formations, and to the eventual prevention of economic and human loss. Moreover, such rock failures are often triggered and aggravated by earthquake ground shaking, and often constitute a large proportion of the earthquake damage at an affected site. The study of such phenomena is therefore even more important in areas which are also subject to seismic hazard such as the Central Mediterranean area (D'Amico *et al.* 2013).

Studies related to the assessment and mapping of landslide hazard, as well as their vulnerability to earthquake shaking, have increased in recent years (e.g. Guzzetti *et al.* 1999; Jongmans & Garambois 2007; van Westen *et al.* 2008; Günther *et al.* 2013; Vessia & Parise 2013). A first step in understanding the extent and nature of a landslide area is detailed geomorphological mapping, recently also using LIDAR scanning techniques (e.g. Schulz 2007; Jaboyedoff *et al.* 2012). Geophysical and geotechnical investigations provide information about subsurface structures, their elastic and mechanical properties and slip surfaces contributing to landsliding. 2-D and 3-D numerical modelling methods have been well developed in recent years to predict the behaviour of unstable slopes and their response to triggers such as seismic shaking (e.g. Crosta *et al.* 2003; van Asch *et al.* 2007). Such models still require detailed knowledge about the geological, mechanical and hydrological properties of the landslide (Méric *et al.* 2007). Lately, slope and coastal instabilities have also been investigated by recording ambient noise,

and the use of techniques such as H/V (horizontal-to-vertical spectral ratio) analysis, *f–k* analysis, site spectral ratios, polarization analysis, etc. (Del Gaudio *et al.* 2008; Burjánek *et al.* 2010, 2012; Coccia *et al.* 2010; Panzera *et al.* 2012). In particular, single station methods prove to be a very cost effective and rapid way of surveying an area, bypassing the problem of bringing bulky instrumentation into mostly inaccessible areas. H/V measurements yield important insights into resonance behaviour of particular lithomorphologies and geomorphological features, while polarization analysis provides information about particle motion and directivity properties, which in turn may be associated with mechanical vibrational behaviour of large scale structures (Burjánek *et al.* 2012).

In this study, we investigate an area of coastal instability characterized by active lateral spreading, rock sliding and rockfalls, which happens to be situated in an area of coastal land use in the form of an amusement park, and which therefore has solicited further concern. This, and similar areas have been the subject of several previous geological and geomorphological studies (e.g. Farrugia 2008; Magri *et al.* 2008; Devoto *et al.* 2011; Mantovani *et al.* 2013). Here we make use of ambient noise recordings, using a single portable seismograph, and evaluate H/V ratios and polarization characteristics to investigate the dynamic characteristics of features at different stages of the destabilization process. The use of ambient noise measurements has in recent years, become more popular in a wide range of geophysical and seismological applications, such as microzonation studies based on seismic site response (e.g. Lachet *et al.* 1996; Fäh *et al.* 1997; Parolai *et al.* 2004), shallow crustal velocity profiling (e.g. D'Amico *et al.* 2008; Panzera & Lombardo 2013), crustal tomography through noise correlation techniques (e.g. Shapiro *et al.* 2005; Campillo 2006; Curtis *et al.* 2006) and in the study of dynamical behaviour of buildings (Mucciarelli & Gallipoli 2007; Gallipoli *et al.* 2008, 2010). In this study, we attempt to explore what information can be obtained from ambient noise about the dynamic behaviour of different regions of the coastal cliff area. It is hoped that these results will enhance the knowledge gained from previous investigations using different methods, and that subsequent work might lead to a correlation between ambient noise characteristics and the state of instability of coastal features.

2 THE STUDY AREA

The Maltese archipelago is situated in the Central Mediterranean, separated from Sicily by the Malta Channel, which is characterized by shallow sea depths of not more than 200 m. The islands are composed of a four-layer sequence of Oligocene–Miocene limestones and clays, with the compact Lower Coralline Limestone (LCL) being the oldest exposed layer, and forming steep sided cliffs along the southern coast of the island. In order of decreasing age, the next three layers are the Globigerina Limestone, a fine-grained foraminiferal limestone; the Blue Clay (BC) formation, a series of carbonate-poor clays and marls that is highly erodible and plastic when wet; and the Upper Coralline Limestone (UCL), a reef limestone that is similar to the LCL and forms a well-developed karst landscape (Pedley *et al.* 1978, 2002, and references therein). In the eastern half of the archipelago, the upper two layers are absent, resulting in a relatively flat landscape of Globigerina limestone outcrop, while the western half of Malta, and the smaller island of Gozo retain the full sedimentary sequence in most places, the landscape consisting characteristically of high UCL plateaux, below which the Blue Clay may run out as taluses forming 45° slopes (Fig. 1).

The study area is located along the northwestern coast of the island of Malta (Fig. 1), forming the northern part of an inlet known as Anchor Bay. The inlet owes its shape to tectonic processes, its southern side being controlled by a normal fault that forms part of an extensive horst-and-graben system characterizing the archipelago north of the Great Fault, or Victoria Lines fault. Throughout this area, the geomorphology is mostly dictated by the fact that the UCL forms a rigid rock slab resting on a much weaker layer of clayey material. This geological situation creates stresses in the upper slab resulting in fracturing and brittle collapse (Gigli *et al.* 2012). When the exposure of the geological cross-section is along the coast, the additional weathering effect of marine processes accelerates the destabilization by erosion of the clay layer. This results in the formation of large cliff-parallel surface fractures, that produce partially isolated blocks having volumes of the order of thousands of cubic metres. Horizontal and vertical mass movement of such blocks forming part of the cliff face, and boulder detachment and collapse, result in a fractured and boulder-strewn coastline, that is typical of much of the northwest coast of Malta (Fig. 2d). In the study area, the faulting process has brought the Blue Clay layer down to sea level on the northern side of the fault, thereby accelerating erosion and destabilization of the overlying UCL. This has in turn shaped the formation of Anchor Bay, as well as producing spectacular examples of coastal lateral spreading and rock sliding phenomena. A map of coastal features of the whole area has been compiled by Devoto *et al.* 2012 (Fig. 1c).

The area investigated in this study covers approximately 0.07 km^2 and is located on the headland known as *Il-Prajjet*, forming the northern part of Anchor Bay. Four main block types—A, B, C and D, have been identified for ambient noise characterization, as shown in Fig. 2. Block type A, represented in Fig. 2 by A1 and A2, consists of large units forming the cliff edge, in an early stage of detachment, separated from the mainland by visible deep fractures reaching 50 cm width in places (Fig. 2b). Numerous other fractures characterize the cliff edge area. Along the E–W trending cliff face, lateral spreading has resulted in one block, B (of area approximately 1400 m^2) being partly detached and lowered vertically by about 2.5 m (Fig. 2c) while another block (block C) has undergone vertical downsliding by about 18 m, and is fractured into about eight smaller fragments (Fig. 2c). Block D is the inland plateau area.

Anchor Bay and *Il-Prajjet* headland have been the subject of a number of studies (e.g. Magri *et al.* 2008; Devoto *et al.* 2011; Mantovani *et al.* 2013). One of the motivations for such detailed studies is the presence of an amusement park (ex-Popeye film set, known locally as Popeye Village) lying directly beneath the cliff (Fig. 2a). A real risk is therefore present, with the non-negligible potential of economic and even human loss. Mantovani *et al.* (2013) have carried out a multidisciplinary study consisting of long-term monitoring using GPS benchmarks and fissure meters, together with geophysical surveys [resistivity tomography and ground penetrating radar (GPR)] to investigate the subsurface structure. Their monitoring results over a 5-yr period indicate vertical and horizontal displacements of blocks B and C of up to 27 mm yr^{-1}, with block B showing the largest vertical displacement, indicating ongoing subsiding. Resistivity tomography and GPR have revealed a gently dipping UCL-BC interface at about 13 m depth. The authors interpret the mass movements in the block sliding area in terms of sliding over a dipping contact interface between the UCL and the BC.

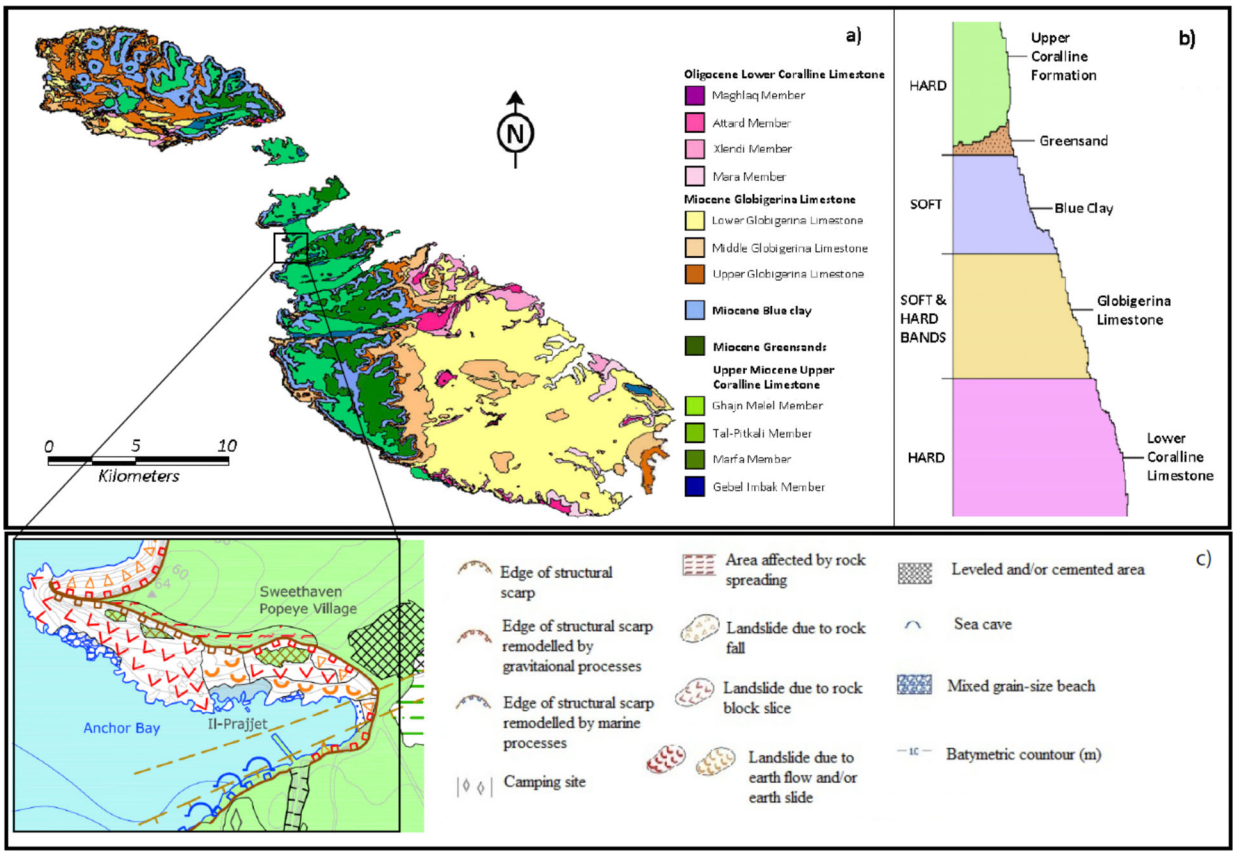

Figure 1. (a) Geological outcrop map of the Maltese islands; (b) representation of the full sedimentary sequence making up the Maltese rocks above sea level; (c) geomorphological map of Anchor Bay area and Il-Prajjet headland, showing the area of study (modified from Devoto *et al.* 2012).

3 METHODOLOGY AND ANALYSIS

Ambient noise measurements were taken at 32 points over an area of approximately 0.07 km^2, covering a wide range of geomorphological states of the area and different stages of rock spreading and cliff collapse, starting from the inland plateau area and moving towards the fractured area close to the cliff edge, as well as directly on vertically displaced blocks. Ambient noise was recorded using a three-component seismometer (Tromino^{TM}, www.tromino.eu). The Tromino is a compact, lightweight and self-contained instrument, and its ease of use makes it ideal for performing a large number of measurements in rugged terrain that are accessible only on foot. Time-series of 20 min each were recorded at a sampling rate of 128 Hz and, following the guidelines suggested by the SESAME project (Bard 2005) these were divided into 60 non-overlapping time windows of 20 s each. The Fourier spectrum of each window was computed and smoothed, and after 'cleaning' the traces from spurious noise event windows, the resulting H/V, in the frequency range 0.5–64.0 Hz, was derived using the geometric mean of the spectral ratio obtained for each time window.

The use of the H/V method was first proposed by Nogoshi & Igarashi (1971) for the estimate of seismic site response. Nakamura (1989) eventually made this method widely popular as a cost-effective and reliable means of predicting the resonance frequency of a site, particularly when low shear-wave velocity layers present a sharp impedance contrast with the bedrock. The presence of a resonance peak in the H/V ratio has been interpreted both in terms of *SH*-wave resonance in soft surface layers, or in terms of the ellipticity of particle motion when the ambient noise wave train is made up predominantly of surface waves (Bonnefoy-Claudet *et al.* 2006). In practice, the wavefield is expected to be a combination of both types, and the H/V curve contains information about the shear wave velocity profile in shallow sediments.

Polarization analysis was carried out using the method of Burjánek *et al.* (2010) which is based on the complex covariance matrix method of particle motion polarization analysis, and generalized to the time-frequency domain by adopting a continuous wavelet transform (CWT). The particle motion is characterised at a given time and frequency by an ellipse in 3-D space. The WAVE-POL package outputs the analysis of an ambient noise time-series in visual representations of combined angular and frequency dependence. Histograms of strike of the ellipse major axis are represented as circles on a polar plot, in which the frequency increases along the radius, and colour is used to denote amplitude in each histogram. The ellipticity of the particle motion is defined as the ratio of the semi-minor axis to the semi-major axis of the ellipse, and is therefore equal to 1 for circular particle motion and equal to zero for purely linear motion, and is thus a good indicator of polarization effects. It is represented as a 3-D histogram of ellipticity versus frequency.

4 RESULTS AND DISCUSSION

4.1 H/V analysis

Fig. 3 shows a summary of the H/V results obtained, grouped by areas of different geomorphological character and degrees of stability. Notable characteristics may be identified for each area.

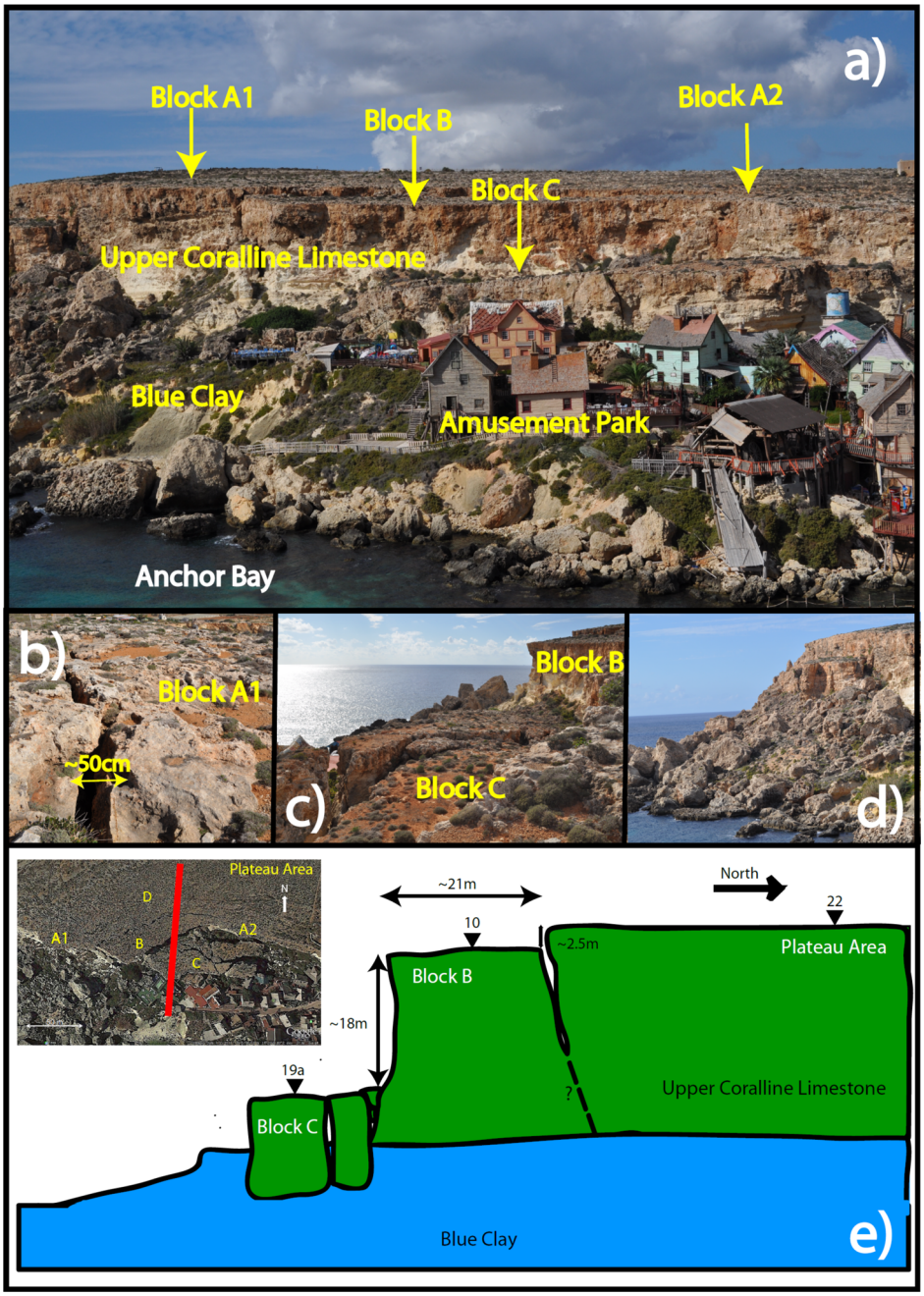

Figure 2. The study area. (a) General view of the area, showing the Popeye film set below the collapsing cliff edge, and identification of blocks A1, A2, B, C; (b) a major fracture separating block A1 from the plateau; (c) a view of the vertically subsided blocks B and C; (d) UCL boulders that have rolled down to the shoreline. The Blue Clay is seen forming an approximately 45° slope; (e) cartoon sketch of cross section across the edge of the cliff, illustrating vertical displacements of blocks B and C, and approximate positions of measurement sites 22, 10 and 19 (modified from Mantovani *et al.* (2013)). The approximate transect is shown on the inset map.

The first important observation is the presence of a ubiquitous resonance peak at between 1.0 and 2.0 Hz. This is not surprising because previous ambient noise studies have repeatedly confirmed that all areas of the Maltese islands where UCL outcrops and is underlain by a layer of Blue Clay exhibits a peak in the H/V of this consistent frequency (Panzera *et al.* 2012, 2013; Vella *et al.* 2013). The clay layer in the Maltese archipelago reaches thicknesses of more than 50 m in the west, and thins as a layer towards the east. Where it is exposed along slopes, it is subjected to considerable erosion and thinning. Fig. 4(a) shows H/V curves from similar geology (UCL overlying BC) at various sites over the Maltese islands, all showing a clear peak between 1.0 and 2.0 Hz, and a dip in the spectral ratio below 1.0 over a wide frequency range. Di Giacomo *et al.* (2005) and Castellaro & Mulargia (2009) interpret this dip in the H/V ratio in terms of a shallow shear-wave velocity inversion, which in this case corresponds to the interface between the UCL and BC. The interpretation of other features of this peak in terms of Rayleigh wave ellipticity and/or trapping of *SH* waves in the low-velocity layer is the subject of an ongoing study using numerical modelling.

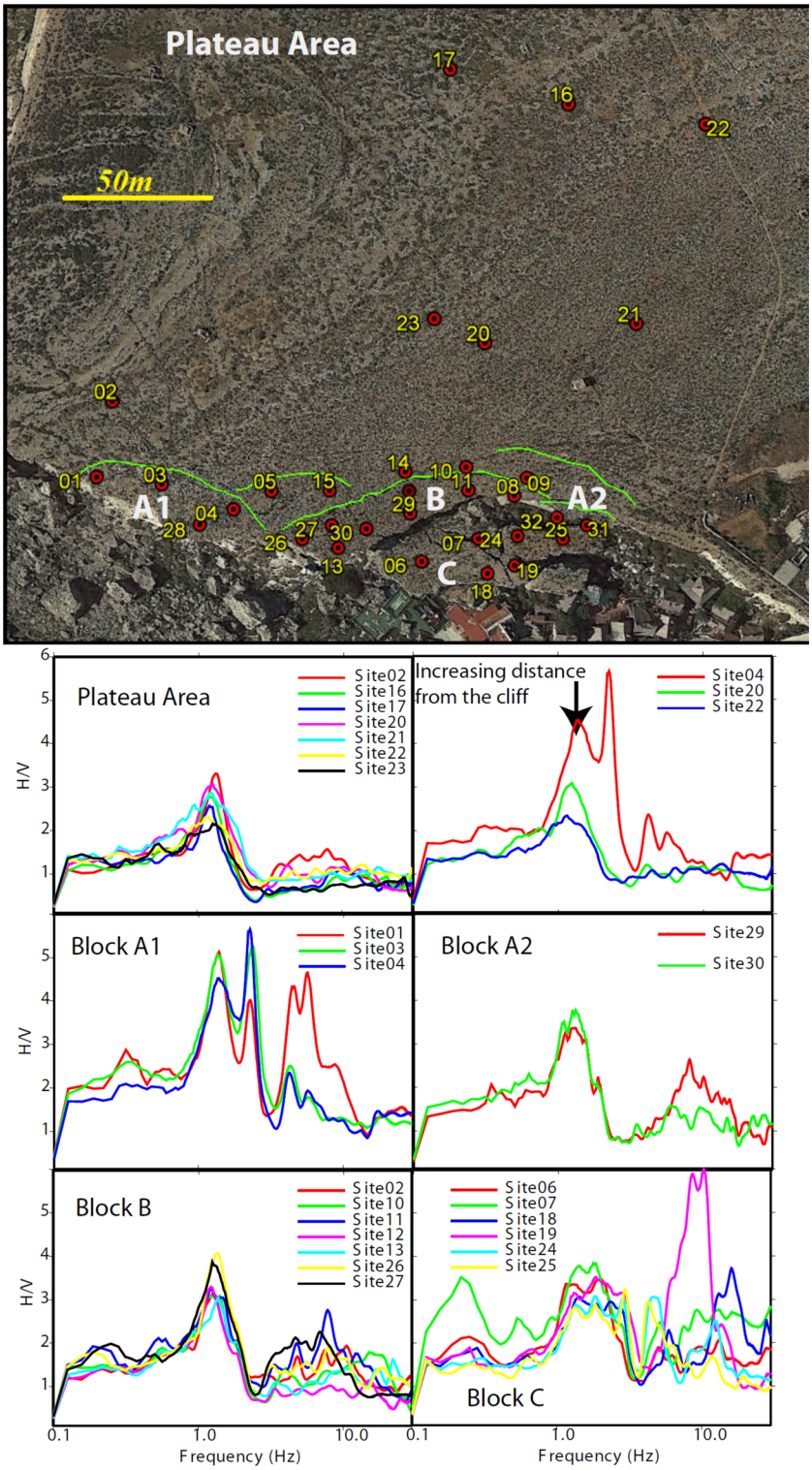

Figure 3. Location of measurement sites and summary of H/V results on the different blocks. The top right graph panel shows the increase in amplitude of the H/V peak at 1.5 Hz on moving from the plateau to the fractured region close to the cliff edge.

Moving from the inland area towards the cliff edge and rock sliding area, the nature of the H/V response changes strikingly. On the plateau away from the cliff edge, the site response shows only the simple and consistent peak at around 1.5 Hz as described above, while the rest of the H/V amplitudes remain at a level well below 2.0 (top left graph panel). Moreover, it is observed that, in general, the amplitude of the peak increases on moving from the plateau area to the cliff edge (top right graph panel). On block types A, the 1.5 Hz peak is retained but pronounced new resonances at well-defined and consistent frequencies are developed. Block A1 shows a major peak at ≈2.4 Hz, with amplitudes exceeding 5.0, and smaller peaks at ≈4.5 and 5.5 Hz., while the smaller block A2 shows a major

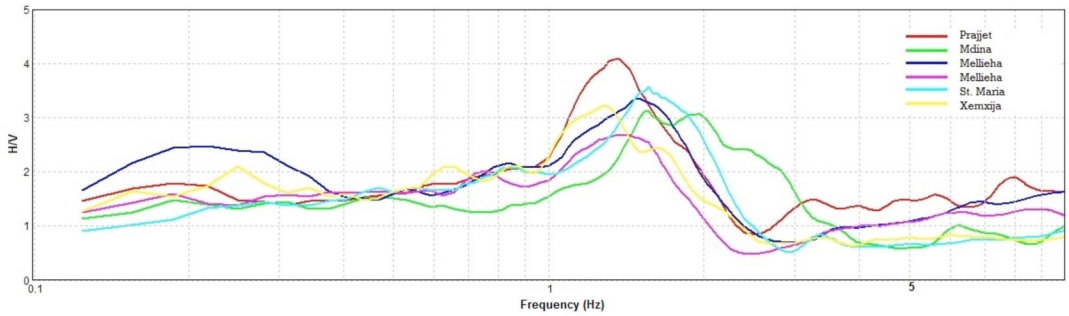

Figure 4. H/V curves, measured during previous surveys, at various points on the Maltese islands with similar subsurface geology to the study area, that is UCL overlying BC. The 1–2 Hz peak is evident at all sites.

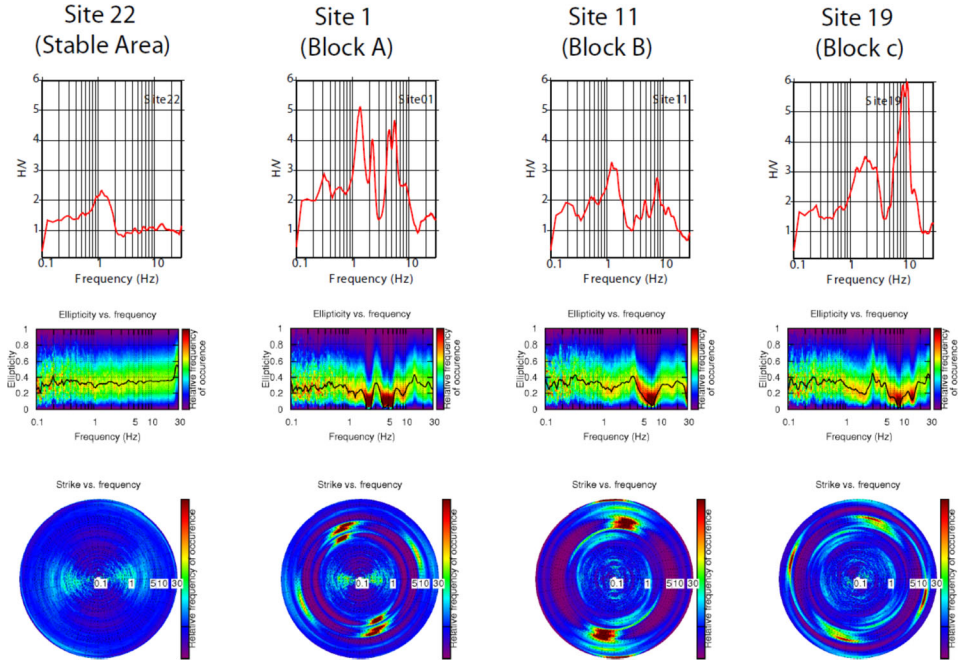

Figure 5. Comparison of H/V and polarisation analysis (ellipticity and strike) for five sites lying on four different blocks. The analysis is for frequencies up to 30 Hz. In the polar plots, frequency is along the radius of the circle.

resonance frequency at 4–5 Hz, reaching an amplitude of 6.0, and a second resonance at 9–10 Hz. Such frequencies, not observed on the plateau area, may be tentatively associated with mechanical vibration modes of the whole blocks.

Block B, undergoing active spreading, shows more complex resonance behaviour. The 1.5 Hz peak persists, while multiple peaks are developed, whose frequencies are not consistent throughout the block, implying complex behaviour due to internal fracturing of the block. Moreover, although some of these H/V peaks have an amplitude that exceeds 2.0, most of them are of low amplitude, implying vertical and horizontal spectra peaks of comparable amplitude, as opposed to the case of the lithologically controlled H/V peak at 1.5 Hz. Finally, the vertically subsided block C (rock sliding area) is visibly fragmented into a number of individual blocks, with H/V curves showing evidence of independent resonance behaviour, while the 1.5 Hz peak becomes broader and less dominant, possibly 'contaminated' by new peaks.

4.2 Polarization analysis

Examples of polarization analysis are presented in Fig. 5, in which the top row shows the H/V curves, the middle row shows the ellipticity-frequency plots, and the bottom row shows the frequency-azimuth polar plots, at five different sites, lying on different terrains. Taken together, these diagrams give a clear picture of the particle motion behaviour in the different areas. Site 22 is on the stable inland area (plateau). The 1.5 Hz peak is not associated with any particular polarization direction, consistently with the fact that this resonance is associated with random-direction sources of ambient noise, and that the peak is due to the subsurface layering. Peaks above 2.0 Hz on all other sites, however, show strong directivity properties at sharply defined frequencies between 2.0 and 10.0 Hz. Site 01, on the partly detached block A1, shows a very sharp peak in H/V at around 2.5 Hz and a sharp double peak between 4.0 and 6.0 Hz. The polarization analysis shows strong characteristics in direct correspondence with these H/V peak frequencies. The polar plot shows directivity of particle motion approximately N340E, while the ellipticity diagram shows a corresponding sharp drop to zero at the same frequencies, indicating a high degree of linearity in the particle motion. On the contrary, the peak at 1.5 Hz is associated with only a slight downward peak in the ellipticity. This appears to be related to the fact that the softer BC layer is buried under the UCL, since it has been observed that the corresponding peak at sites where BC outcrops at the surface produces larger dips

in the ellipticity, however never to the same extent as the linearity observed in this study at the higher frequencies. At the same site, a smaller peak at 9.0 Hz shows directivity in an orthogonal direction, although less linearity. The above differences, in particular the linearity and directivity characteristics, appear to confirm that these higher frequency resonances correspond to mechanical vibrational modes of this particular block, and are distinct from the persistent 1.5 Hz resonance.

Similar observations apply to other sites along the cliff edge. Site 11 on block B shows very strong directional resonance at frequencies between 3.0 and 11.0 Hz, oriented approximately northeast, and with strongly linear motion. However, the H/V peaks are not so pronounced at these frequencies. Site 19a, which is on the vertically subsided, and detached block C, shows clear H/V peaks at around 10.0 Hz, which separate in the polar plot into two distinct and orthogonal directions of resonance at N15E and N105E, both of which show linear properties. This is interesting to observe because this block is practically detached from the cliff face and therefore is able to vibrate in different directions. This observation is true for other points on this block.

It should be noted that a mechanical vibration mode, although clearly identified in terms of polarization strike and linearity, need not necessarily exhibit an H/V resonance peak, the reason being that such modes may show individual maxima of all spectral components (vertical and two horizontals) at these frequencies, as opposed to the stratigraphy-related peaks (in this case the 1.0–2.0 Hz peak) for which the individual spectra form an 'eye-shape' due to the lowering of the vertical spectra with respect to the horizontal ones (Castellaro & Mulargia 2009). Fig. 6 shows an example of such behaviour at Site 10, which lies very close to the edge of the cliff. Here the maximum polarization intensity occurs at 6.0–10.0 Hz and between N350E and N05E, while at these frequencies, no particularly pronounced H/V peaks are observed. This indicates that these frequencies represent particular modes of vibration with a significant vertical component spectrum (hence preventing a peak in H/V), such as rocking modes, as observed in the bottom panel.

Fig. 7 shows the main directions of polarization at all sites for frequencies up to 10.0 Hz. There is a general consistency between the directions of polarization within individual blocks, being generally aligned at right angles to the cliff edge. It is interesting to observe that sites 5 and 15, which appear to lie on a minor block identified by visible surrounding fractures, display a predominant polarization in an E–W direction, in contrast to adjacent blocks, implying independent behaviour of this block. Similarly, sites 26 and 13 on block B, appear to imply an independently oscillating block, as confirmed also by a visible fracture seen down the vertical face of block B. On the rock sliding area, where blocks are fully detached from the cliff face and fragmented into separate blocks, there was less consistency between directions of polarization.

For frequencies above 10.0 Hz, the results are more difficult to interpret. H/V peaks around 30.0 Hz are common, but do not show consistency in polarization characteristics, and will not be interpreted here.

On comparing the results of polarization analysis with the results obtained from GPS monitoring (Mantovani *et al.* 2013) over the last 5 yr, we observe that the directions revealed by the two methods do not quite coincide (blue arrows in Fig. 7). The GPS monitoring reveals a consistent sliding of about 24 mm yr^{-1} towards the southwest on the rock spreading area (block B) and a general sliding towards the south in the block sliding area C. A significant downward vertical movement of up to 10.9 cm is also reported on block B during a 5-yr period, while hardly any vertical lowering has been observed on

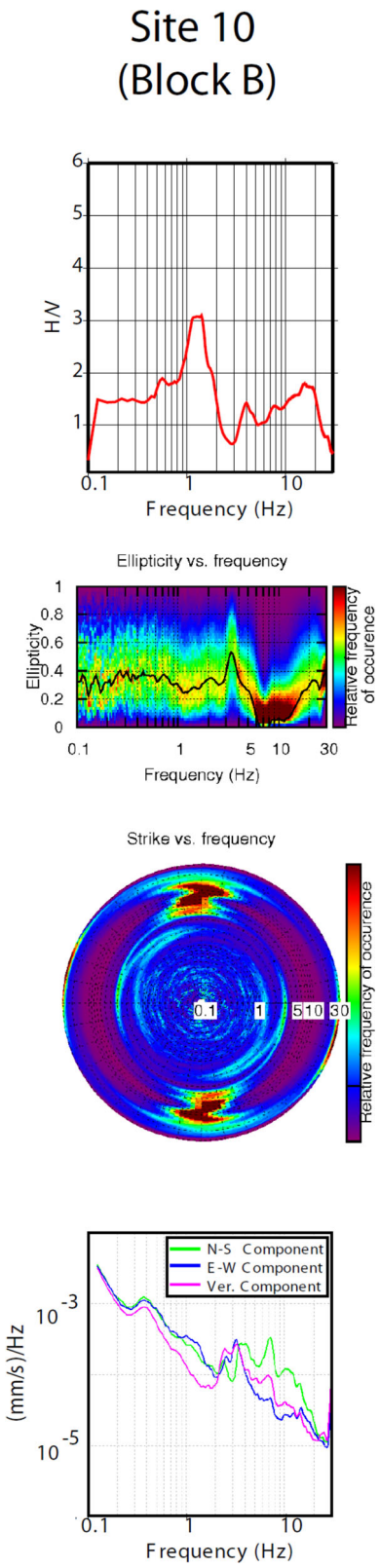

Figure 6. Example of H/V graph, polarization analysis and individual spectra at site 10, for which strong polarization occurs at specific frequencies, with no corresponding H/V peaks.

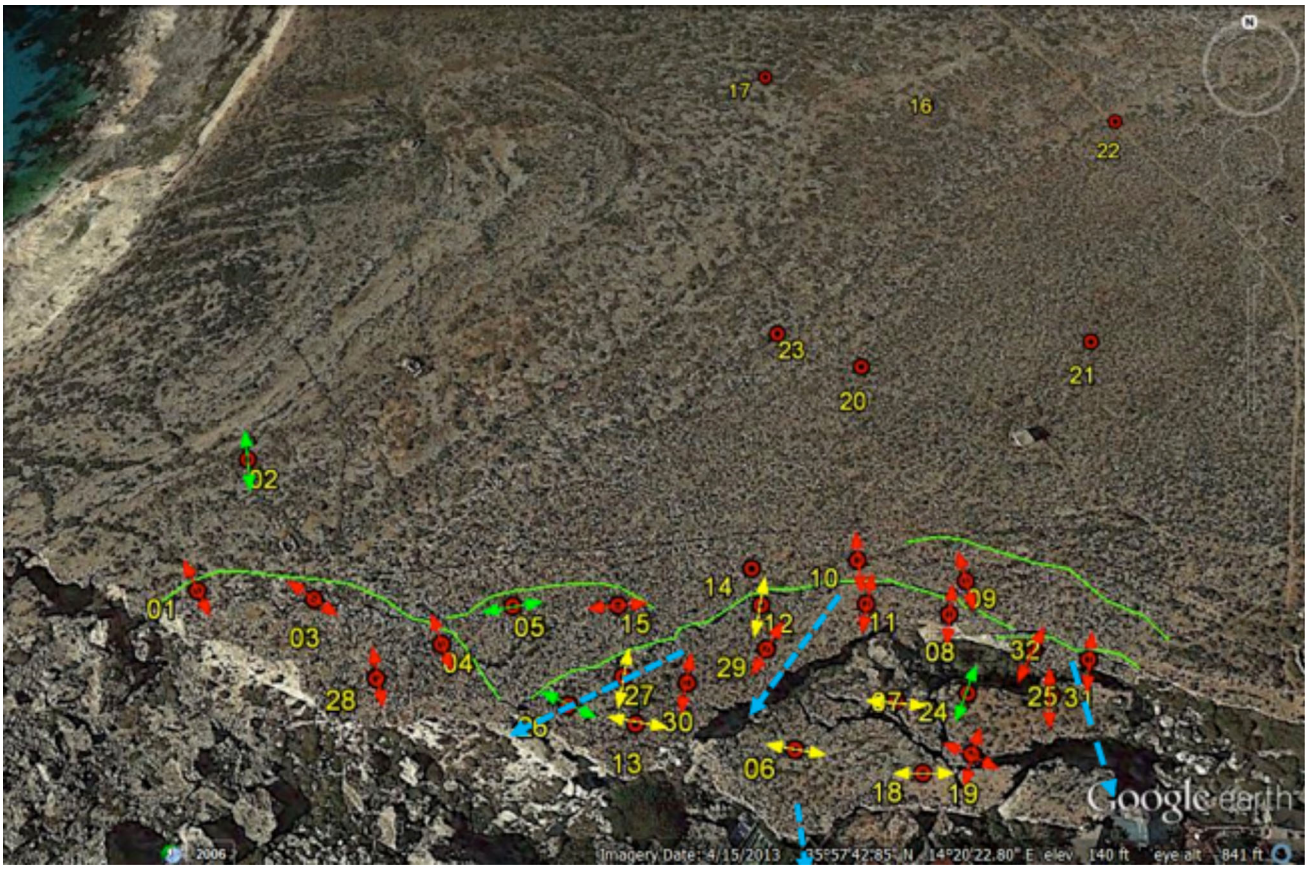

Figure 7. Main polarisation directions at measurement sites for frequencies up to 10 Hz. The colours indicate the intensity of the polarization effect, as defined by the colour scale in Fig. 5. The dashed, light blue arrows represent the directions of motion as inferred from GPS measurements in Mantovani *et al.* (2013).

block C. The authors interpret these directions in terms of sliding of the blocks in the direction of inclination of the bedrock–clay interface. Our polarization analyses, on the other hand, do not represent long-term mass movements but high frequency modal vibrations which reflect the degrees of freedom of individual blocks, although possibly sliding in a common direction occurs in the longer term.

5 CONCLUSION

Ambient vibration time-series have been shown to contain information that is relevant to the behaviour of coastal features at different stages of destabilisation. Using polarisation analysis, it has been possible to distinguish unambiguously between H/V peaks that are related to the shallow crustal layering, including a prominent low-velocity layer in this particular case, and higher frequency peaks that are evidently related to mechanical behaviour of detached masses.

The higher frequencies are intuitively related to mechanical vibrational modes. Where blocks are only partly detached from the mainland, and are limited in their degrees of freedom, the dominant direction of polarization (at frequencies up to 10.0 Hz) is generally normal to the cliff edge, or to the large scale fractures. Where blocks are fully detached, the polarization directions appear to indicate the existence of more degrees of freedom. The ellipticity variable that is output from the polarization analysis is a highly indicative parameter that confirms the linearity of particle motion associated with normal mode vibration, this linearity being absent in the stratigraphically derived H/V peaks at 1.0–2.0 Hz. The amplitude of H/V peaks likewise appears to vary with the state of the particular block structure. Large amplitudes are exhibited on blocks A1 and A2, which are in a state of early detachment, indicating strong horizontal translational motion. Other sites, in particular sites on block B which is undergoing vertical sliding, produce smaller, or no H/V peaks, but clearly polarized and linear particle motion at well-defined frequencies, or frequency bands, indicating that both horizontal and vertical components are present in the modes.

Although not the principal object of investigation here, the 1–2 Hz peaks raise some interesting questions that merit further investigation vis-a-vis their relationship with the buried soft layer, such as the lack of a significant associated dip in the ellipticity as expected from Rayleigh wave behaviour (see e.g. Konno & Ohmachi 1998), the increase in amplitude on moving to areas of more fractured UCL, and the dip in H/V below 1.0 at frequencies beyond the main peak. In particular it is relevant to ask whether they are best interpreted in terms of Rayleigh wave ellipticity and/or trapped body waves in the low-velocity layer, what is the contribution of higher mode Rayleigh waves, and the influence of the negative impedance contrast at the top of the BC. The investigation of such features through numerical modelling will be the subject of further studies.

The results from this study agree very well with those obtained by Burjánek *et al.* (2012) in their study of an unstable rock slope in the southern Swiss Alps. On the basis of polarization analysis, the authors conclude that the wavefield within the potentially unstable rock mass is dominated by normal mode vibration rather than randomly generated surface wave microtremor. The amplification in the unstable area was shown to be strongly directional and oriented perpendicularly to tension cracks.

In the case of the Swiss Alps, the observed normal mode frequencies were centred around 1.6 Hz, and thus significantly lower than those obtained in this study. This is probably due to the larger dimensions of the unstable structures in the Alps, which produce lower resonance frequencies.

The identification of normal mode behaviour of unstable rock masses, coupled with increased directional amplification, has implications for the hazard assessment of seismically induced mass movements. It would be interesting to investigate whether high-amplitude modal response of particular blocks may identify those features which are most likely to collapse in the near future. Blocks with strong horizontal translational modes, with clearly defined frequencies, may be particularly susceptible. The susceptibility to collapse of unstable blocks at the cliff edge as a function of earthquake ground motion parameters, such as, for example, Arias intensity (Lenhardt 2007) should also be investigated further, especially since this type of scenario is a very common setting along the north west coast of Malta, the island of Gozo, and inland cliff top localities of similar lithostratigraphy. Historically, occurrence of rockfalls directly related to earthquake shaking has been reported on cliffs with similar geology, for example 1693 and 1743 (Galea 2007). In recent years, such environments are becoming increasingly subject to land use, both residential and recreational, and this makes it particularly important to investigate more deeply the phenomenon of seismically induced landslides in the Maltese islands.

ACKNOWLEDGEMENTS

The authors are grateful to J. Burjanek for the use of the polarization codes. We also thank the two anonymous reviewers whose insightful comments helped to improve the manuscript.

REFERENCES

Bard, P.Y., 2005. Guidelines for the implementation of the H/V spectral ratio technique on ambient vibrations: measurements, processing, and interpretations, *SESAME European Research Project*. WP12, deliverable D23.12, 2004, Available at: http://sesame-fp5.obs.ujf-grenoble.fr/Deliverables2004.

Bonnefoy-Claudet, S., Cotton, F. & Bard, P.Y., 2006. The nature of noise wavefield and its applications for site effects studies: a literature review, *Earth-Sci. Rev.,* **79**(3), 205–227.

Burjánek, J., Gassner-Stamm, G., Poggi, V., Moore, J.R. & Fäh, D., 2010. Ambient vibration analysis of an unstable mountain slope, *Geophys. J. Int.,* **180**(2), 820–828.

Burjánek, J., Moore, J.R., Yugsi Molina, F.X. & Fäh, D., 2012. Instrumental evidence of normal mode rock slope vibration, *Geophys. J. Int.,* **188**(2), 559–569.

Campillo, M., 2006. Phase and correlation in random seismic fields and the reconstruction of the Green function, *Pure appl.Geophys.,* **163,** 475–502.

Castellaro, S. & Mulargia, F., 2009. The effect of velocity inversions on H/V, *Pure appl. Geophys.,* **166**(4), 567–592.

Coccia, S., Del Gaudio, V., Venisti, N. & Wasowski, J., 2010. Application of refraction microtremor (ReMi) technique for determination of 1-D shear wave velocity in a landslide area, *J. appl. Geophys.,* **71**(2), 71–89.

Crosta, G.B., Imposimato, S. & Roddeman, D.G., 2003. Numerical modelling of large landslides stability and runout, *Nat. Hazards Earth Syst. Sci.,* **3**(6), 523–538.

Curtis, A., Gerstoft, P., Sato, H., Snieder, R. & Wapenaar, K., 2006. Seismic interferometry—turning noise into signal, *Leading Edge,* **25**(9), 1082–1092.

D'Amico, S., Lombardo, G. & Panzera, F., 2013. Seismicity of the Mediterranean region and mitigation of earthquake losses, *Phys. Chem. Earth,* **63,** 1–2.

D'Amico, V., Picozzi, M., Baliva, F. & Albarello, D., 2008. Ambient noise measurements for preliminary site-effects characterization in the urban area of Florence, Italy, *Bull. seism. Soc. Am.,* **98**(3), 1373–1388.

Del Gaudio, V., Coccia, S., Wasowski, J., Gallipoli, M.R. & Mucciarelli, M., 2008. Detection of directivity in seismic site response from microtremor spectral analysis, *Nat. Hazards Earth Syst. Sci.,* **8,** 751–762.

Devoto, S., Biolchi, S., Bruschi, V.M., González Dıez, A., Mantovani, M., Pasuto, A. & Soldati, M., 2011. Landslides along the north-west coast of the Island of Malta, in *Proceedings of the Second World Landslide Forum,* 3–9 October 2011, Rome.

Devoto, S., Biolchi, S., Bruschi, V.M., Furlani, S., Mantovani, M., Piacentini, D. & Soldati, M., 2012. Geomorphological map of the NW Coast of the Island of Malta (Mediterranean Sea), *J. Maps,* **8**(1), 33–40.

Di Giacomo, D., Gallipoli, M.R., Mucciarelli, M., Parolai, S. & Richwalski, S.M., 2005. Analysis and modelling of HVSR in the presence of a velocity inversion: the case of Venosa, Italy, *Bull. seism. Soc. Am.,* **95**(6), 2364–2372.

Fäh, D., Rüttener, E., Noack, T. & Kruspan, P., 1997. Microzonation of the city of Basel, *J. Seismol.,* **1**(1), 87–102.

Farrugia, M.T., 2008. Coastal erosion along northern Malta: geomorphological processes and risks, *Geografia Fisica e Dinamica Quaternaria,* **31**(2), 149–160.

Galea, P., 2007. Seismic history of the Maltese islands and considerations on seismic risk, *Ann. Geophys.,* **50,** 725–740.

Gallipoli, M.R., Mucciarelli, M. & Vona, M., 2008. Empirical estimate of fundamental frequencies and damping for Italian buildings, *Earthq. Eng. Struct. Dyn.*, **38**(8), 973–988.

Gallipoli, M.R., Mucciarelli, M., Šket-Motnikar, B., Zupančić, P., Gosar, A., Prevolnik, S. & Olumćeva, T., 2010. Empirical estimates of dynamic parameters on a large set of European buildings, *Bull. Earthq. Eng.,* **8**(3), 593–607.

Gigli, G., Frodella, W., Mugnai, F., Tapete, D., Cigna, F., Fanti, R. & Lombardi, L., 2012. Instability mechanisms affecting cultural heritage sites in the Maltese Archipelago, *Nat. Hazards Earth Syst. Sci.,* **12,** 1883–1903.

Günther, A., Van Den Eeckhaut, M., Malet, J.-P., Reichenbach, P. & Hervás, J., 2013. European Landslide Susceptibility Map (ELSUS1000) Version 1 Methodology. Technical note, 14.02.2013. European Soil Portal, Available at: http://eusoils.jrc.ec.europa.eu (last accessed 10 July 2014).

Guzzetti, F., Carrara, A., Cardinali, M. & Reichenbach, P., 1999. Landslide hazard evaluation: a review of current techniques and their application in a multi-scale study, Central Italy, *Geomorphology,* **31**(1–4), 181–216.

Jaboyedoff, M., Oppikofer, T., Abellán, A., Derron, M.H., Loye, A., Metzger, R. & Pedrazzini, A., 2012. Use of LIDAR in landslide investigations: a review, *Nat. Hazards,* **61**(1), 5–28.

Jongmans, D. & Garambois, S., 2007. Geophysical investigation of landslides: a review, *Bulletin de la Société géologique de France,* **178**(2), 101–112.

Konno, K. & Ohmachi, T., 1998. Ground-motion characteristics estimated from spectral ratio between horizontal and vertical components of microtremor, *Bull. seism. Soc. Am.,* **88**(1), 228–241.

Lachet, C., Hatzfeld, D., Bard, P.Y., Theodulidis, N., Papaioannou, C. & Savvaidis, A., 1996. Site effects and microzonation in the city of Thessaloniki (Greece) comparison of different approaches, *Bull. seism. Soc. Am.,* **86**(6), 1692–1703.

Lenhardt, W.A., 2007. Earthquake-triggered landslides in Austria–Dobratsch revisited, *Jahrbuch der Geologischen Bundesanstalt,* **147**(1), 193–199.

Magri, O., Mantovani, M., Pasuto, A. & Soldati, M., 2008. Geomorphological investigation and monitoring of lateral spreading along the north-west coast of Malta, *Geografia Fisica e Dinamica Quaternaria,* **31**(2), 171–180.

Mantovani, M., Devoto, S., Forte, E., Mocnik, A., Pasuto, A., Piacentini, D. & Soldati, M., 2013. A multidisciplinary approach for rock spreading and block sliding investigation in the north-western coast of Malta, *Landslides,* **10**(5), 611–622.

Méric, O., Garambois, S., Malet, J.P., Cadet, H., Guéguen, P. & Jongmans, D., 2007. Seismic noise-based methods for soft-rock landslide

characterization, *Bulletin de la Societe Geologique de France,* **178**(2), 137–148.

Mucciarelli, M. & Gallipoli, M.R., 2007. Non-parametric analysis of a single seismometric recording to obtain building dynamic parameters, *Ann. Geophys.,* **50,** 259–266.

Nakamura, Y., 1989. A method for dynamic characteristics estimation of subsurface using microtremor on the ground surface, Quarterly Report of Railway Technical Research Institute (RTRI), Vol. 30, No. 1, pp. 25–33.

Nogoshi, M. & Igarashi, T., 1971. On the amplitude characteristics of microtremor (part 2), *J. Seismol. Soc. Japan,* **24,** 26–40.

Panzera, F. & Lombardo, G., 2013. Seismic property characterization of lithotypes cropping out in the Siracusa urban area, Italy, *Eng. Geol.,* **153,** 12–24.

Panzera, F., D'Amico, S., Lotteri, A., Galea, P. & Lombardo, G., 2012. Seismic site response of unstable steep slope using noise measurements: the case study of Xemxija Bay area, Malta, *Nat. Hazards Earth Syst. Sci.,* **12**(11), 3421–3431.

Panzera, F., D'Amico, S., Galea, P., Lombardo, G., Gallipoli, M.R. & Pace, S., 2013. Geophysical measurements for site response investigation: preliminary results on the island of Malta, *Bollettino di Geofisica Teorica ed Applicata,* **54**(2), 111–128.

Parolai, S., Richwalski, S.M., Milkereit, C. & Bormann, P., 2004. Assessment of the stability of H/V spectral ratios from ambient noise and comparison with earthquake data in the Cologne area (Germany), *Tectonophysics,* **390,** 57–73.

Pedley, H.M., House, M.R. & Waugh, B., 1978. The geology of the Pelagian block: the Maltese islands, in *The Ocean Basins and Margins,* pp. 417–433, eds Nairn, A.E.M., Kanes, W.H. & Stehli, F.G., Plenum Press.

Pedley, M., Hughes-Clarke, M. & Galea, P., 2002. *Limestone Isles in a Crystal Sea—The Geology of the Maltese Islands,* Publishers Enterprises Group Ltd.

Schulz, W.H., 2007. Landslide susceptibility revealed by LIDAR imagery and historical records, Seattle, Washington, *Eng. Geol.,* **89**(1), 67–87.

Shapiro, N.M., Campillo, M., Stehly, L. & Ritzwoller, M.H., 2005. High-resolution surface-wave tomography from ambient seismic noise, *Science,* **307**(5715), 1615–1618.

van Asch, T.W., Malet, J.P., van Beek, L.P. & Amitrano, D., 2007. Techniques, issues and advances in numerical modelling of landslide hazard, *Bulletin de la Société géologique de France,* **178**(2), 65–88.

van Westen, C.J., Castellanos, E. & Kuriakose, S.L., 2008. Spatial data for landslide susceptibility, hazard, and vulnerability assessment: an overview, *Eng. Geol.,* **102**(3), 112–131.

Vella, A., Galea, P. & D'Amico, S., 2013. Site frequency response characterisation of the Maltese islands based on ambient noise H/V ratios, *Eng. Geol.,* **163,** 89–100.

Vessia, G. & Parise, M., 2013. GIS-based landslide hazard evaluation at the regional scale: some critical points in the permanent displacement approach for seismically-induced landslide maps, in *Proceedings of the EGU General Assembly Conference,* Abstracts, Vol. 15, p. 9250.